ICRANet-Armenia

MULTI-WAVELENGTH STUDY OF HIGH-REDSHIFT BLAZARS

G. HARUTYUNYAN D. ISRAYELYAN

SIXTEENTH MARCEL GROSSMANN MEETING

INTRODUCTION

- **In the unification scheme of radio-loud active galactic nuclei (AGNs) blazars are a subclass with a relativistic jet making a small angle with the observer's line of sight.**

- **Blazars are characterized with high polarization, short and strong variations both in time and amplitude**

- **Blazars are grouped into two large classes: FSRQs and BL Lacs, based on the absence or presence of emission lines in their optical spectra.**

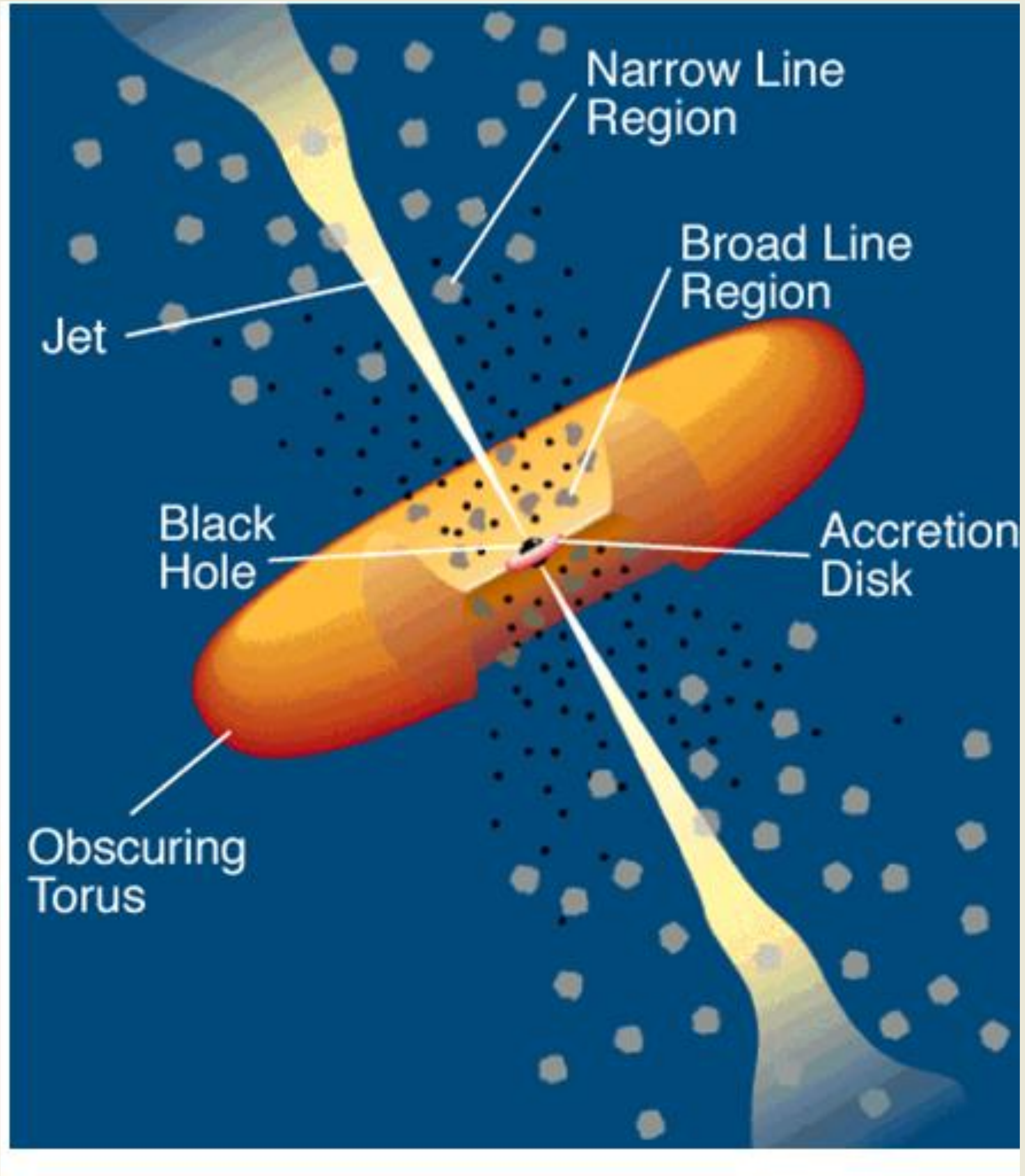

Why z > 2.5?

- Cosmological evolution of blazars and supermassive black holes
- Evolution of relativistic jets across different cosmic epochs
- Limit on the density Extragalactic Background Light
- For studying accretion disc-jet connection
- To investigate environments around supermassive black holes

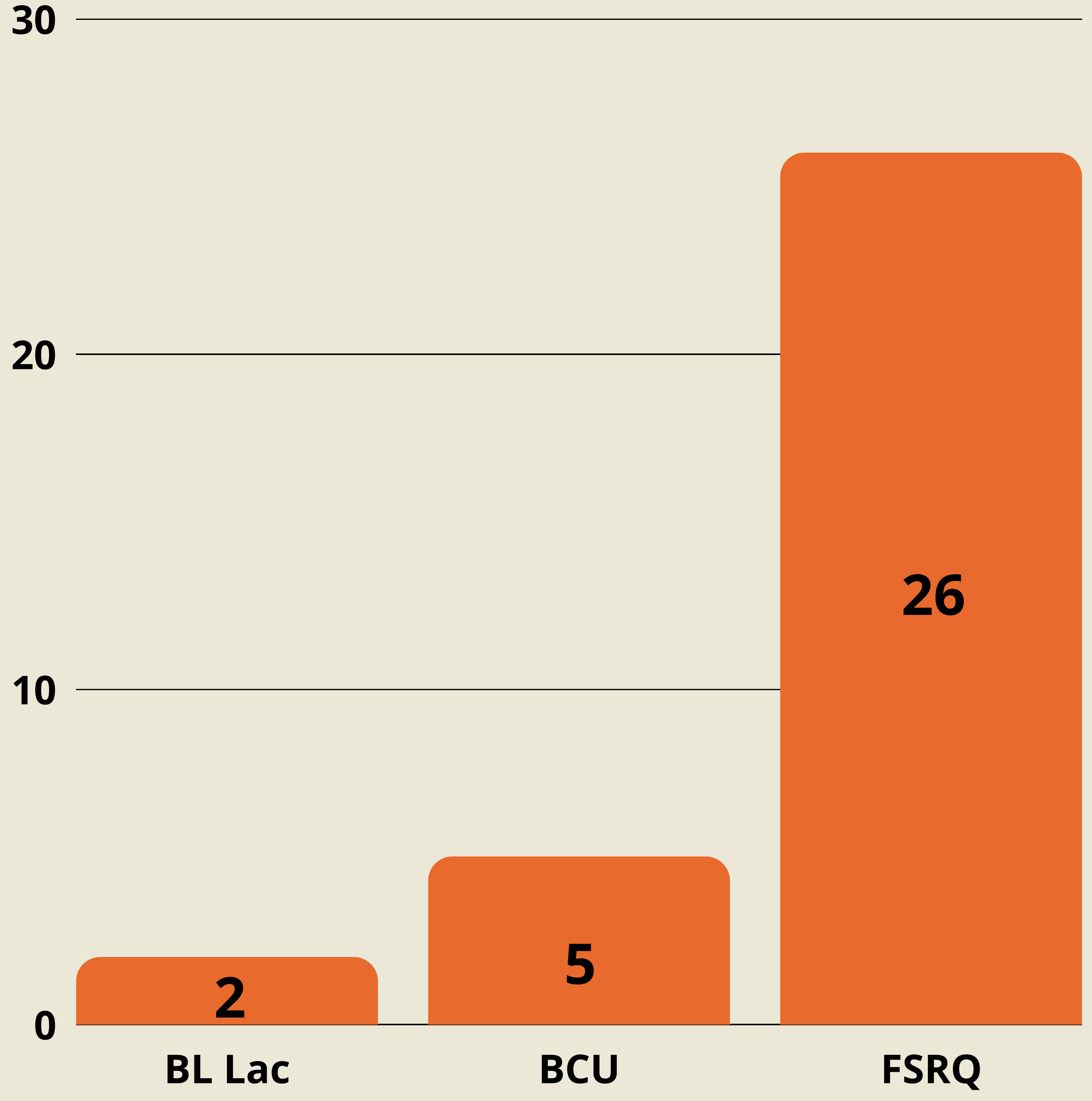

Fermi-LAT Analysis

- Accumulated data 2008-08-04 - 2018-08-04
- Filtered with gtselect and gtmktime
- Binned with gtbin
- Model was generated using 4FGL-DR2
- Maximum-likelihood was implemented with gtlike

Swift Analysis

- All available observations during 15 years
- Swift XRT
  - Source region is a circle with 20 pixel radius
  - Background is an annulus region with 51 and 85 pixels inner and outer radii
  - Fitting was performed with the XPSEC tool.
- Swift UVOT
  - Source region is a circle with 5" radius
  - Background is a circle with 20" radius
  - Uvotsource was used for conversion source counts and after were corrected with reddening coefficients E(B − V) for extinction.

Analysis Results

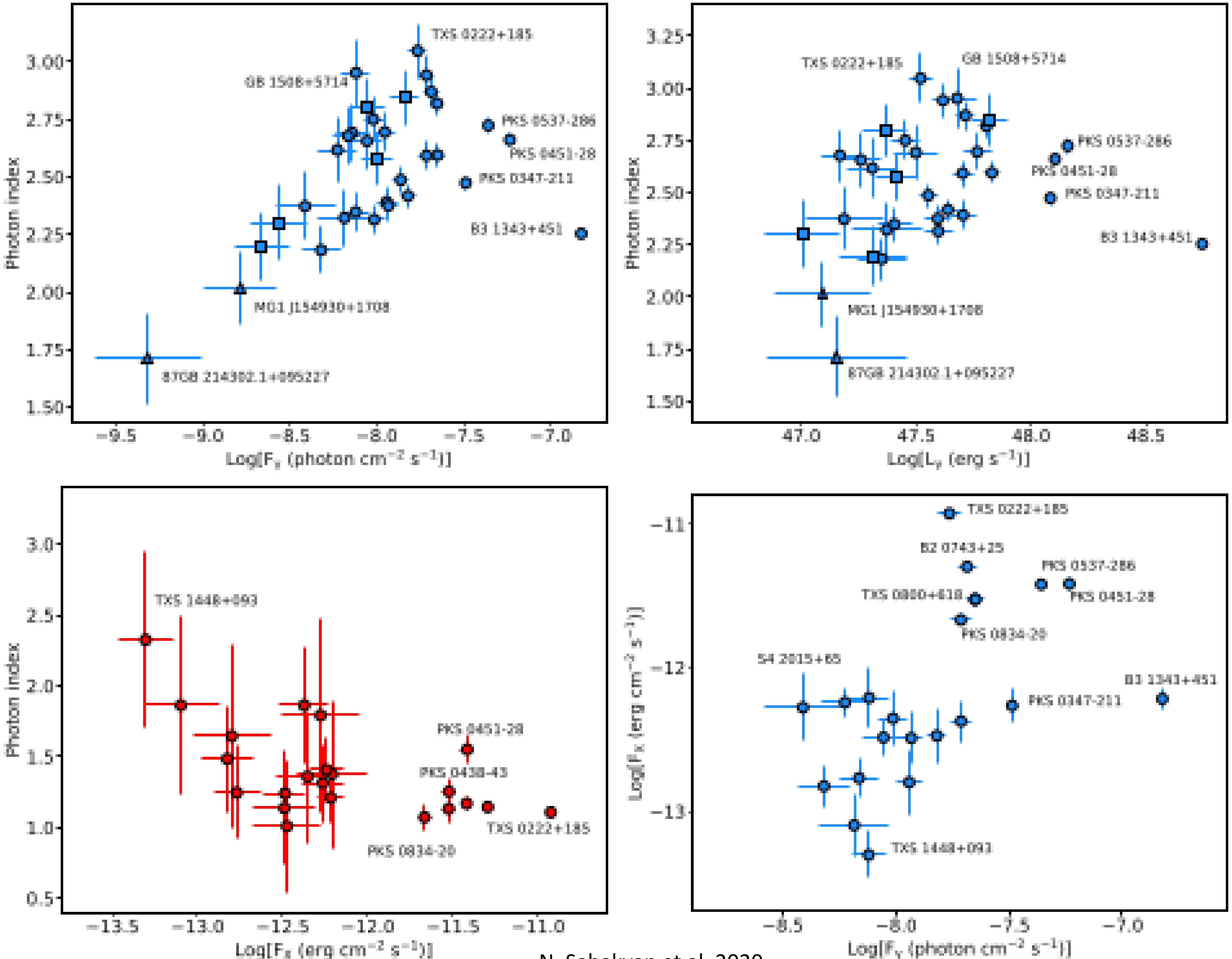

N. Sahakyan et al, 2020

γ-ray	
Photon index	1.71 – 3.05
Flux	$4.84 \times 10^{-10} - 1.5 \times 10^{-7}$ $photon\ cm^{-2}s^{-1}$
Luminosity	$1.01 \times 10^{47} - 5.54 \times 10^{48}$ $erg\ s^{-1}$
X-ray	
Photon index	1.01 – 2.33
Flux	$5 \times 10^{-14} - 10^{-11}$ $erg\ cm^{-2}s^{-1}$

BL Lacs - ▲

FSRQs - ●

BCUs - ■

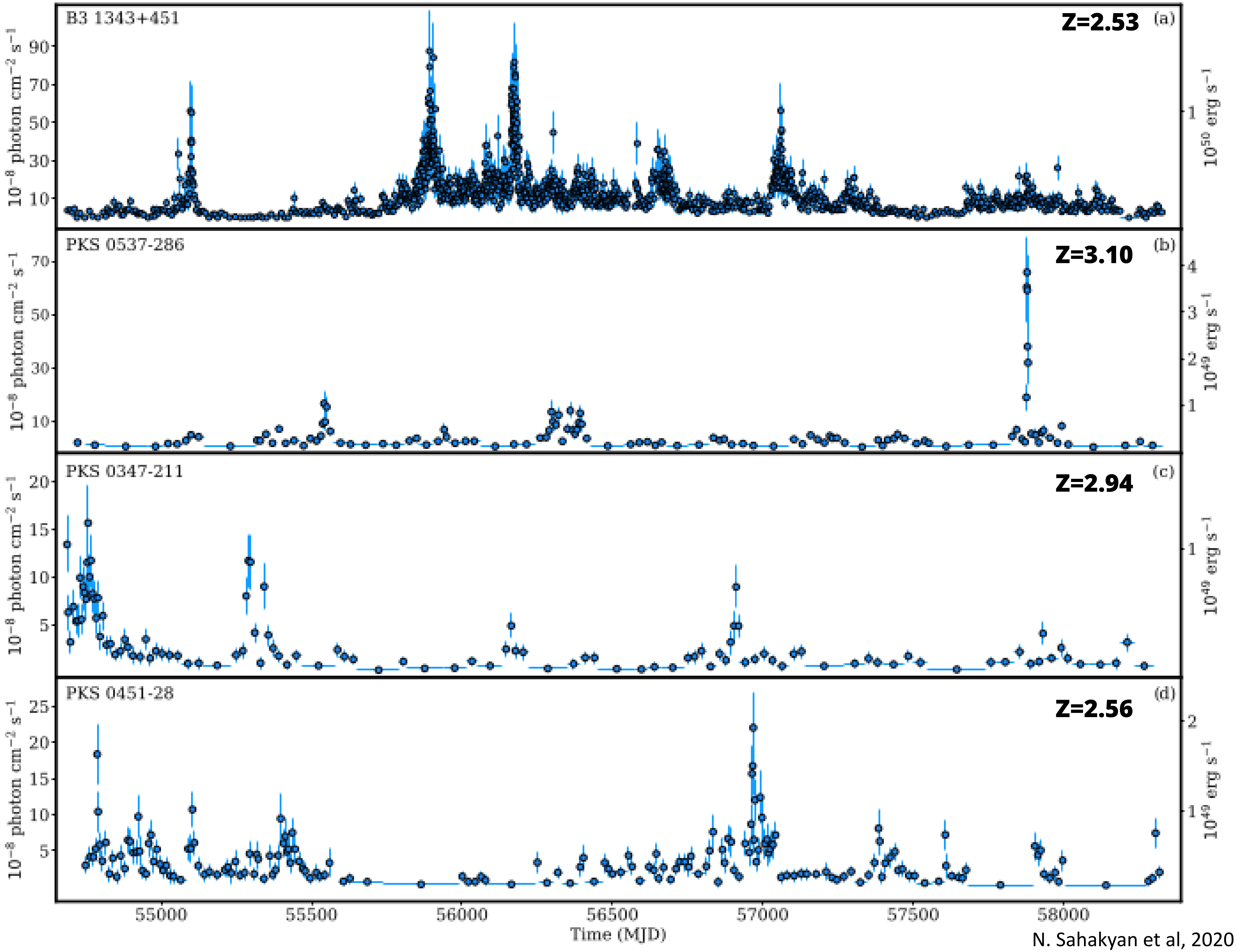

N. Sahakyan et al, 2020

Adaptively binned light curves

1. B3 1343+451
   - quiescent state the γ -ray flux is $\simeq (1-5) \times 10^{-8}\ photon\ cm^{-2}s^{-1}$
   - on MJD 55891.7 was observed the highest γ -ray flux which is $(8.77 \pm 2.16) \times 10^{-7}\ photon\ cm^{-2}s^{-1}$
   - the average luminosity is $(2-4) \times 10^{48} erg\ s^{-1}$

2. PKS 0537-280
   - The average γ –ray flux is $(4.38 \pm 0.18) \times 10^{-8}\ photon\ cm^{-2}s^{-1}$
   - on MJD 57879.2 was observed the highest γ -ray flux which is $(6.58 \pm 1.35) \times 10^{-7}\ photon\ cm^{-2}s^{-1}$

3. PKS 0347-211
   - on MJD 54757.04 ± 2.71 the γ -ray flux was $(1.57 \pm 0.41) \times 10^{-7}\ photon\ cm^{-2}s^{-1}$

4. PKS 0451-28
   - on MJD 56968.60 ± 0.79 the peak γ -ray flux $(2.20 \pm 0.5) \times 10^{-7}\ photon\ cm^{-2}s^{-1}$

Other γ-ray LightCurves

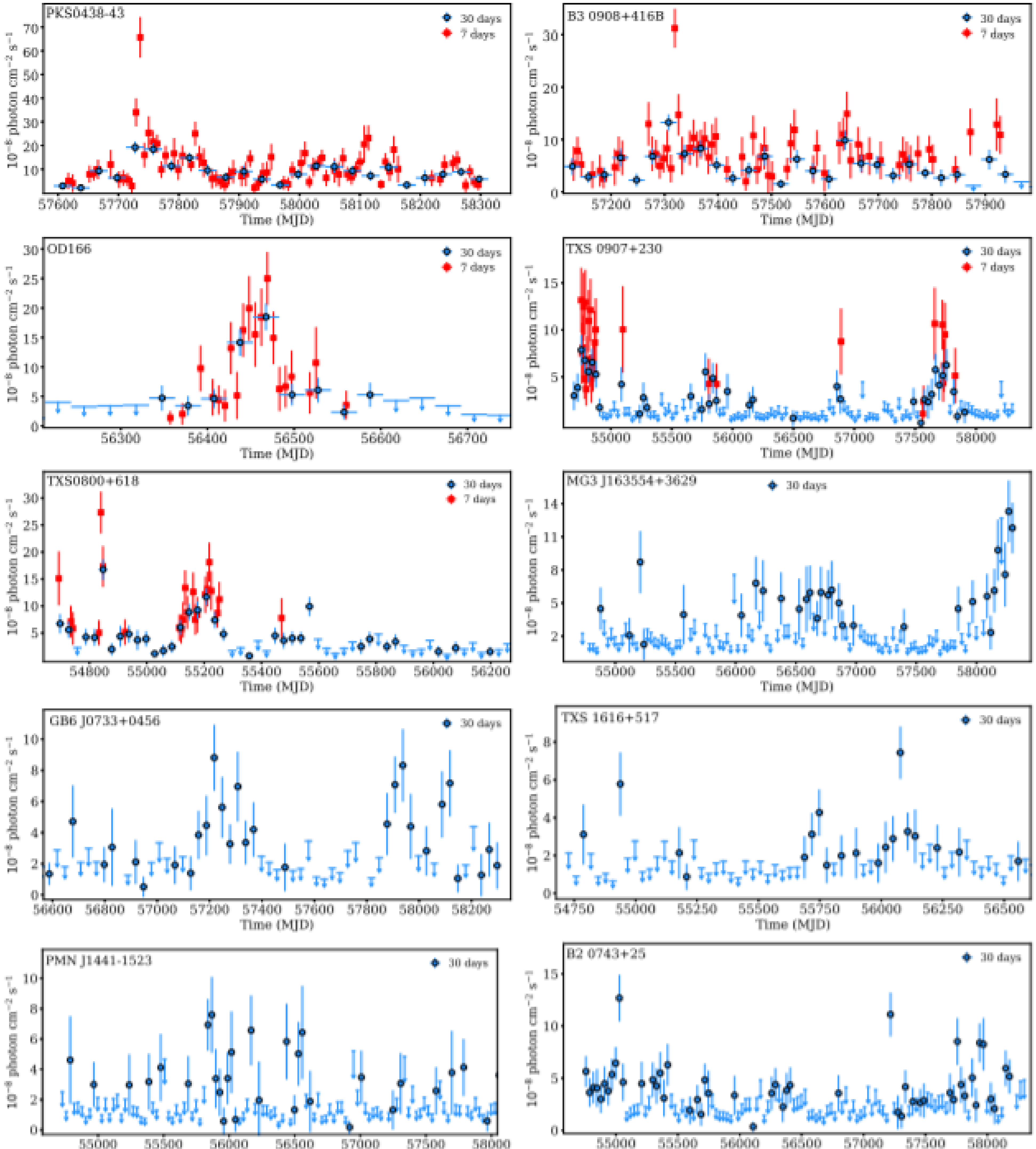

For these sources flux variabilities were

week-month scales

The most distant flaring blazar is MG3 J163554+3629 (z = 3.65). The averaged peak value of γ -ray flux was $(6.4 \pm 1.15) \times 10^{-7}$ photon $cm^{-2} s^{-1}$.

N. Sahakyan et al, 2020

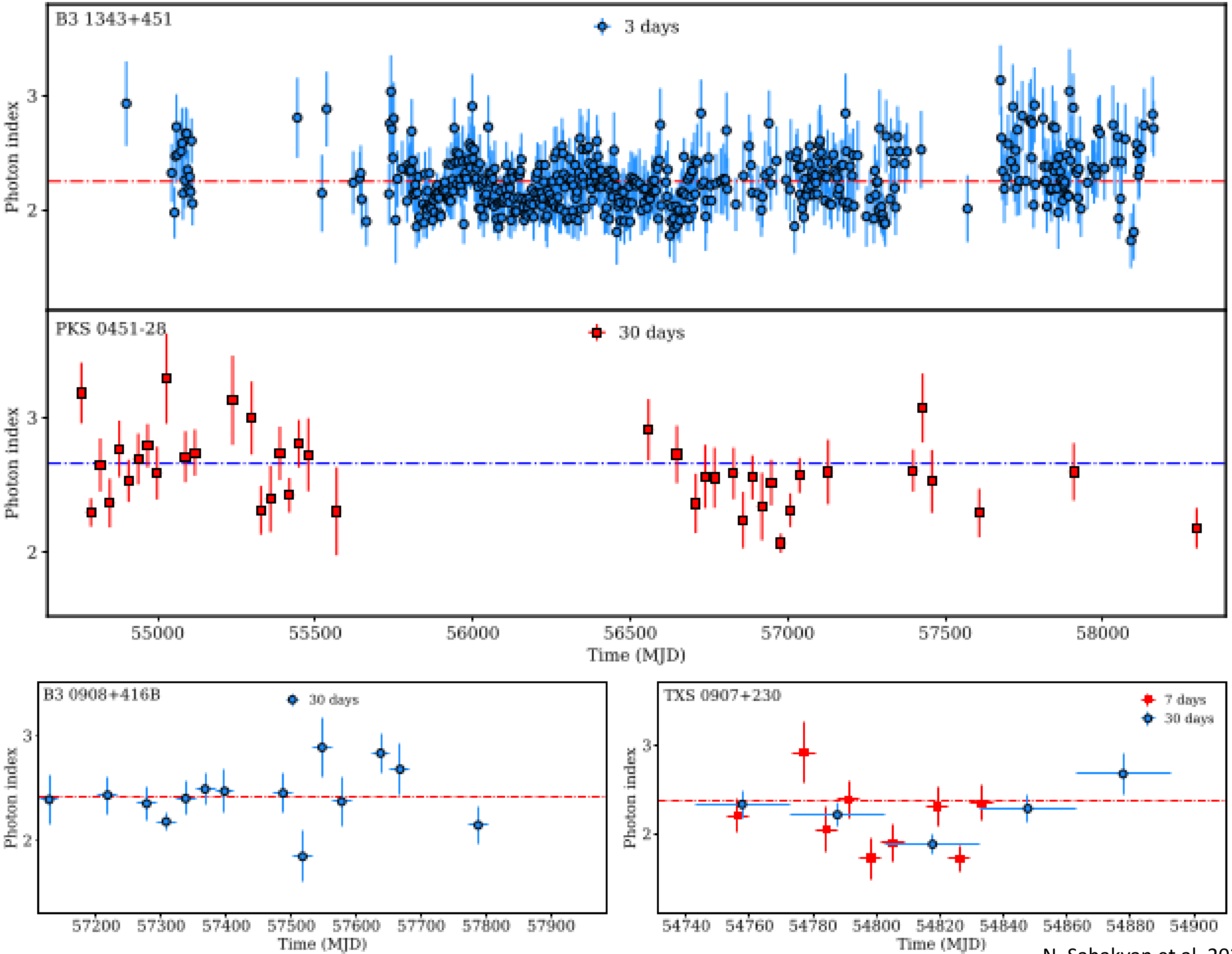

N. Sahakyan et al, 2020

γ-ray photon index variability

- The hardest photon index of $B3\ 1343+451$ was observed on MJD 58089.16 ± 1.5 with $\Gamma_{\gamma} = 1.73 \pm 0.24$.
- In the 30-d binned light curve of $PKS\ 0451-28$ are observed periods when $\Gamma_{\gamma} = 2.06 \pm 0.07$ and $\Gamma_{\gamma} = 2.17 \pm 0.15$ on MJD 56977.66 and 58297.66, respectively.
- The γ-ray spectrum of $B3\ 0908+416B$ averaged over 10 year was 2.42 ± 0.05 meanwhile on MJD 57517.66 the photon index changed to 1.84 ± 0.25.
- The 7-day binned light curve of $TXS\ 0907+230$ shows that there are three periods when its γ-ray emission appears with an unusually hard γ-ray spectrum with $\Gamma_{\gamma} = 1.72 \pm 0.23$, 1.90 ± 0.21 and 1.72 ± 0.15.

Theoretical Modeling

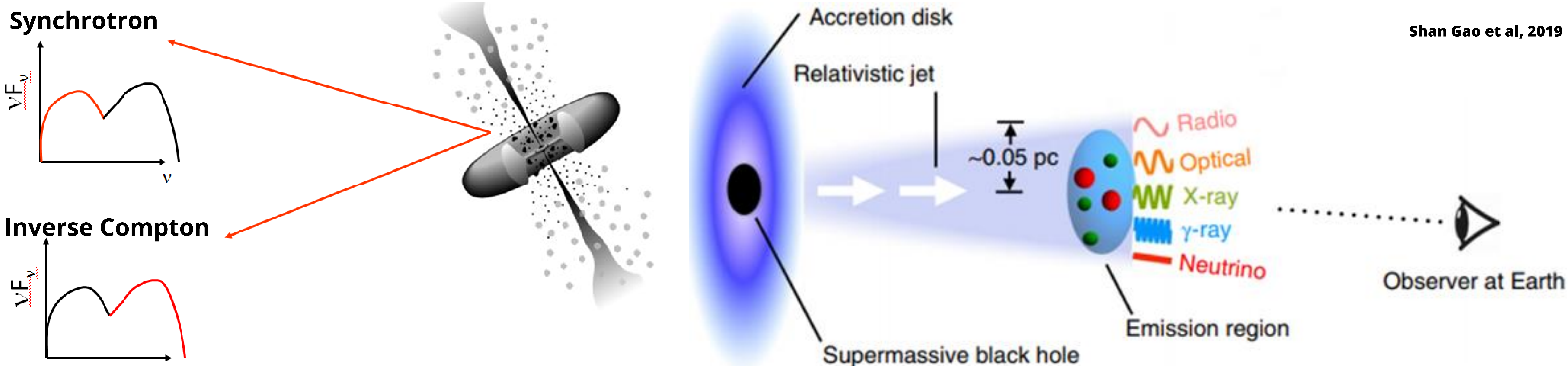

Shan Gao et al, 2019

Have been used one-zone leptonic model

The emission region is assumed to be a spherical blob of radius of R

The emitting region is filled with a uniformly tangled magnetic field B

The emission region contains homogeneous population of relativistic electrons

SED of Bright Sources

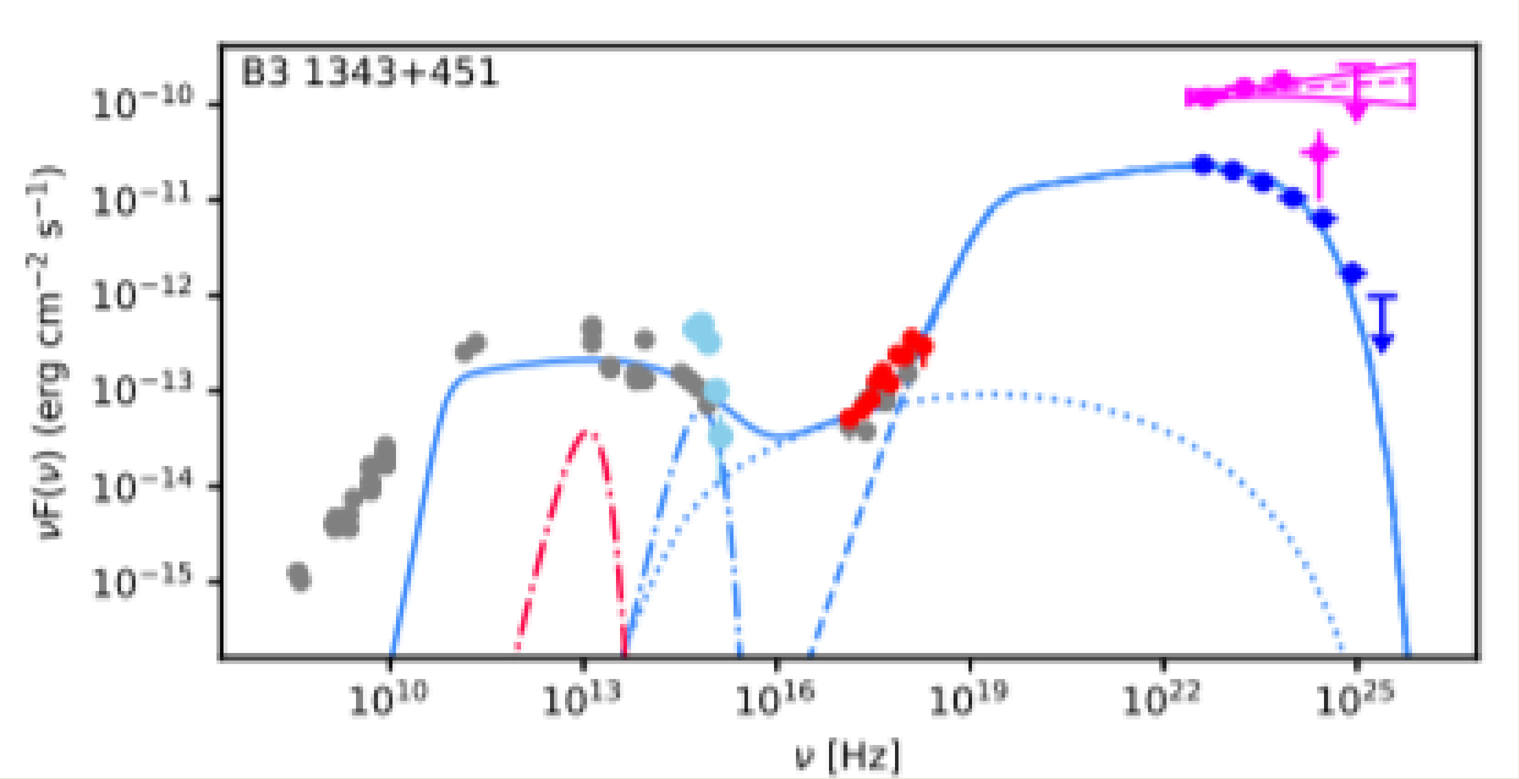

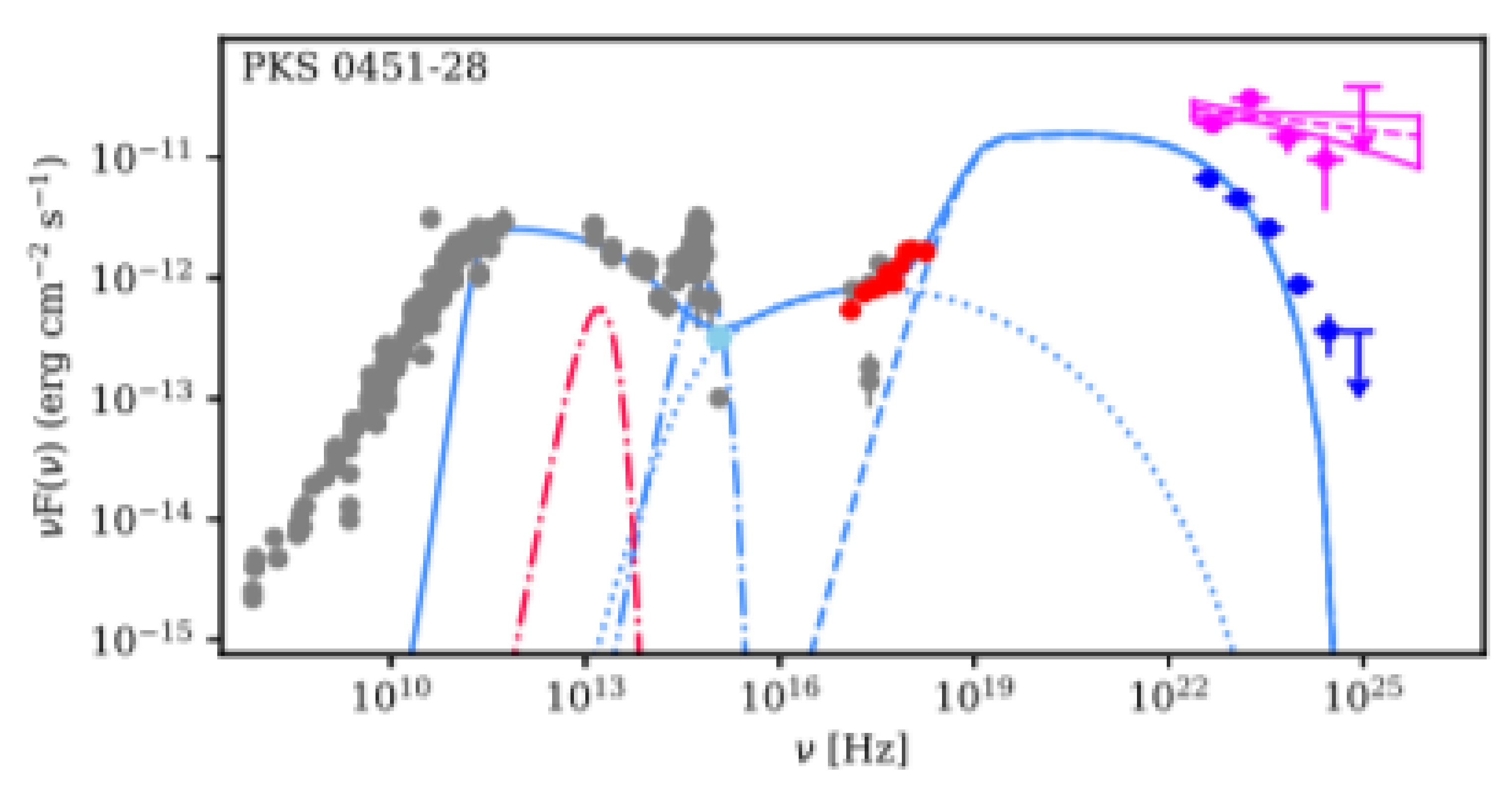

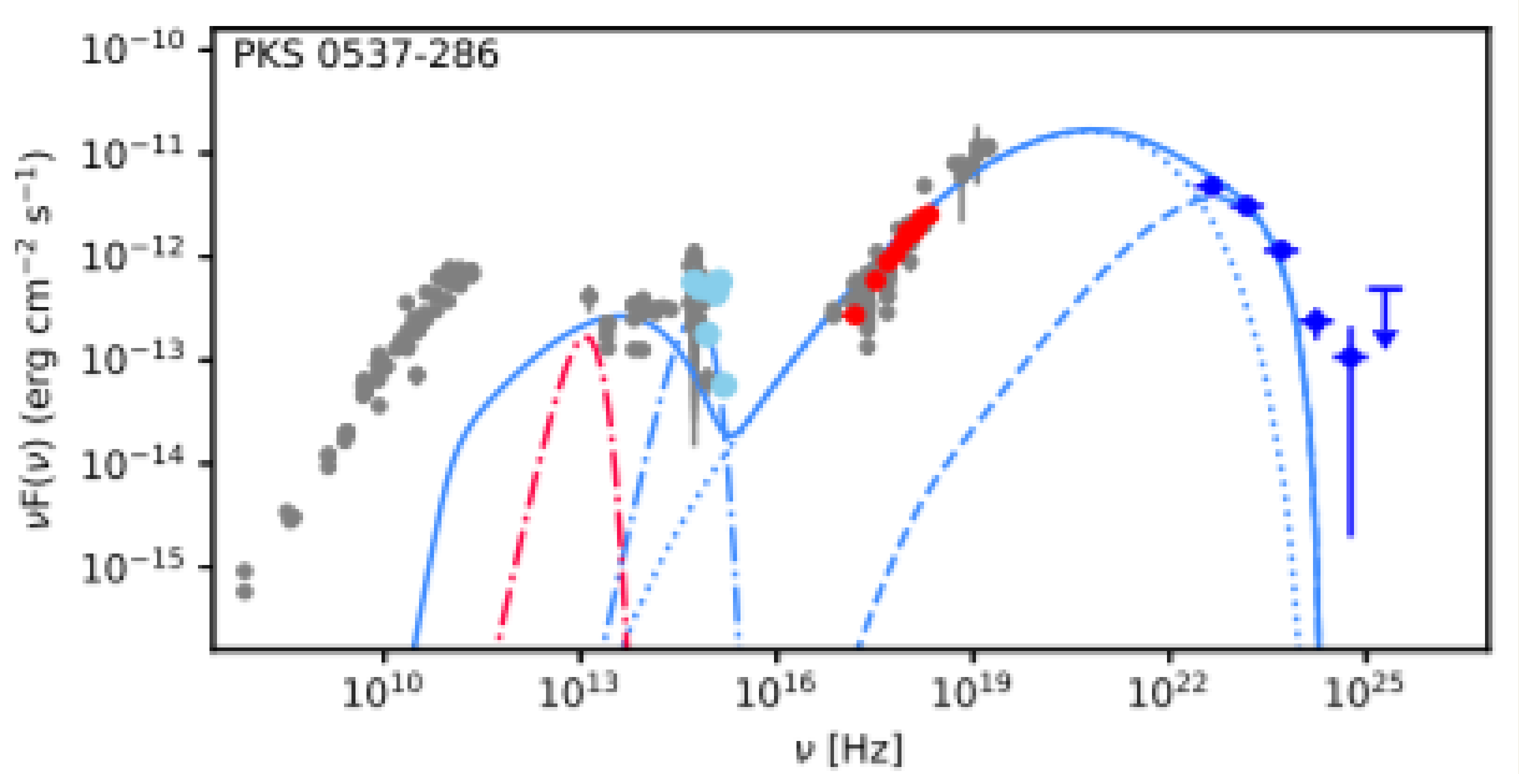

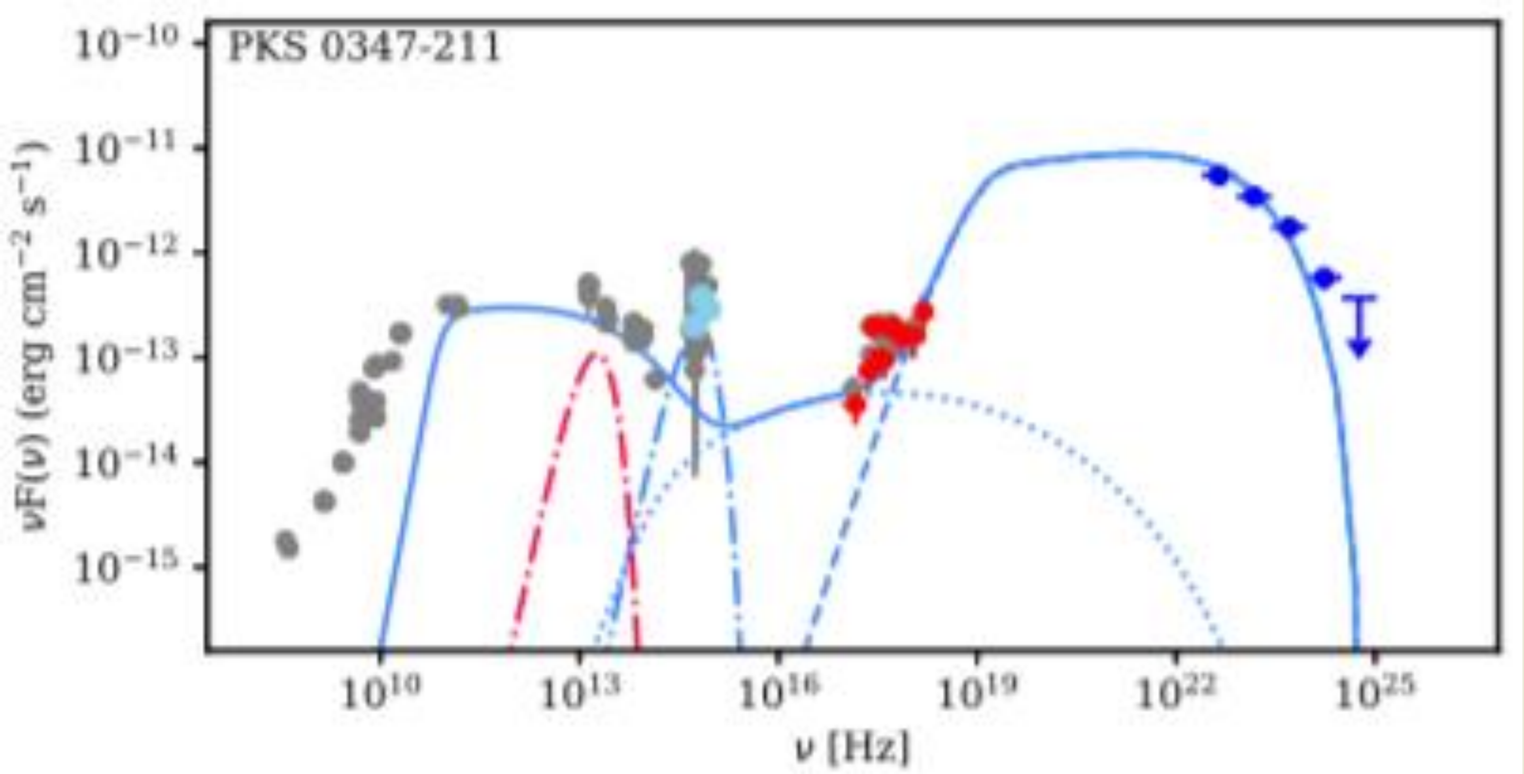

N. Sahakyan et al, 2020

SED of Other Sources

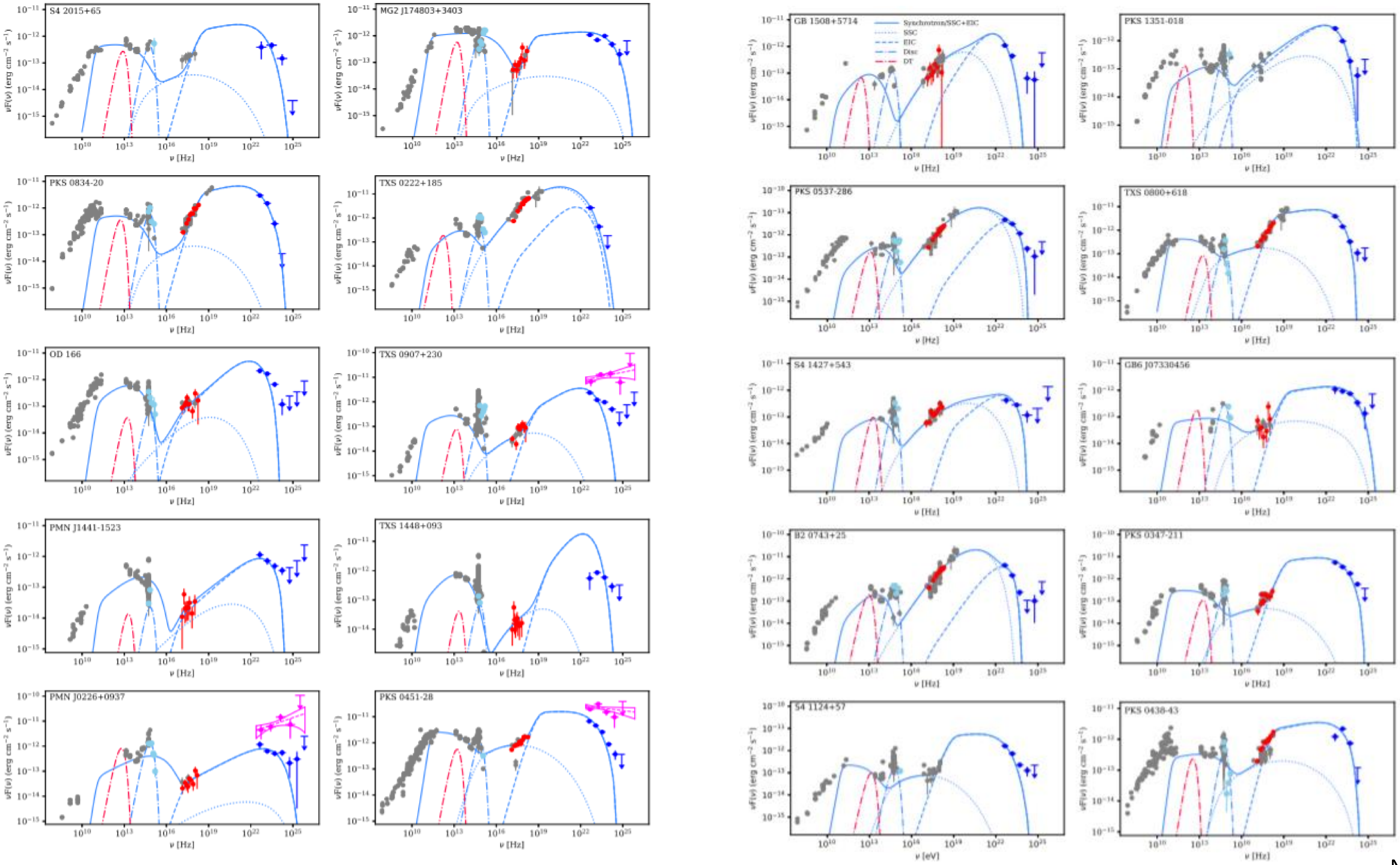

N. Sahakyan et al, 2020

Table of results

Sources [1]	δ [2]	α [3]	γ_{min} [4]	γ_{cut} [5]	B [6]	R [7]	U_e [8]	U_B [9]	L_d [10]	L_e [11]	L_B [12]
GB 1508+5714	15.72 ± 1.29	1.17 ± 0.07	26.90 ± 2.88	1.30 ± 0.10	0.19 ± 0.02	2.28	0.50	1.49	3.02	2.43	0.73
PKS 1351-018	20.47 ± 2.49	2.16 ± 0.11	2.68 ± 0.36	4.99 ± 0.71	0.20 ± 0.02	2.29	0.54	1.66	4.04	2.68	0.82
PKS 0537-286	11.50 ± 0.57	1.33 ± 0.07	15.70 ± 1.49	2.45 ± 0.16	0.28 ± 0.02	1.14	5.93	3.21	3.44	7.31	0.40
TXS 0800+618	14.04 ± 0.56	2.75 ± 0.04	13.98 ± 0.86	2.20 ± 0.02	0.26 ± 0.01	15.5	0.06	2.73	1.65	13.49	61.84
S4 1427+543	10.00 ± 0.37	2.04 ± 0.10	29.00 ± 2.55	2.79 ± 0.27	0.53 ± 0.04	1.90	0.63	10.02	1.83	2.14	3.75
GB6 J0733+0456	16.28 ± 1.36	2.80 ± 0.04	47.90 ± 3.42	15.73 ± 1.60	0.16 ± 0.03	2.98	0.12	6.22	3.40	0.98	5.20
PKS 0347-211	26.00 ± 1.02	2.79 ± 0.02	23.09 ± 1.12	2.62 ± 0.16	0.20 ± 0.01	8.15	0.03	1.61	1.99	1.72	10.08
B2 0743+25	10.02 ± 0.45	1.13 ± 0.19	7.66 ± 0.22	2.03 ± 0.08	0.36 ± 0.01	0.70	16.90	0.003	3.58	7.80	0.24
S4 1124+57	22.17 ± 1.37	2.78 ± 0.04	22.92 ± 1.45	1.28 ± 0.10	0.22 ± 0.01	5.15	0.14	1.95	1.69	3.39	4.87
PKS 0438-43	18.17 ± 1.29	2.78 ± 0.04	23.13 ± 1.54	7.19 ± 0.58	0.34 ± 0.02	5.42	0.12	4.52	3.91	3.33	12.52
S4 2015+65	17.85 ± 1.32	2.73 ± 0.05	20.63 ± 1.64	2.75 ± 0.29	0.46 ± 0.03	13.50	0.07	8.41	4.55	1.26	14.44
MG2 J174803+3403	24.50 ± 2.06	2.87 ± 0.06	14.67 ± 1.58	1.40 ± 0.49	1.45 ± 0.09	7.41	0.004	83.98	8.87	0.23	434.69
PKS 0834-20	27.42 ± 0.97	2.70 ± 0.06	20.57 ± 1.51	2.13 ± 0.18	0.37 ± 0.02	6.83	0.02	5.44	5.51	0.70	23.92
TXS 0222+185	10.03 ± 0.28	1.62 ± 0.05	19.56 ± 0.98	2.38 ± 0.10	0.35 ± 0.02	1.07	10.28	5.04	2.71	11.10	0.54
OD 166	19.02 ± 0.84	1.96 ± 0.04	2.58 ± 0.15	1.01 ± 0.03	1.15 ± 0.05	4.32	0.01	0.52	0.53	0.25	92.38
TXS 0907+230	21.66 ± 1.66	2.23 ± 0.11	20.26 ± 1.84	1.44 ± 0.10	0.31 ± 0.02	5.23	0.03	3.72	1.09	0.70	5.96
PMN J1441-1523	17.01 ± 1.50	2.19 ± 0.07	2.86 ± 0.29	3.31 ± 0.46	1.68 ± 0.14	1.47	0.07	112.38	0.17	0.14	22.85
TXS 1448+093	17.90 ± 1.13	1.52 ± 0.15	49.64 ± 5.82	0.84 ± 0.06	0.70 ± 0.05	7.96	0.003	19.44	0.56	0.17	115.93
PMN J0226+0937	25.02 ± 1.98	2.41 ± 0.04	5.37 ± 0.59	8.32 ± 0.62	1.74 ± 0.12	3.09	0.03	119.86	10.94	0.03	107.98
PKS 0451-28	26.14 ± 1.27	2.90 ± 0.28	21.93 ± 1.3[illegible]	2.19 ± 0.01	0.45 ± 0.03	5.90	0.11	8.01	7.20	3.59	26.32
B3 0908+416B	23.22 ± 1.72	1.31 ± 0.25	6.41 ± 0.72	1.11 ± 0.10	0.39 ± 0.03	1.76	0.09	6.10	0.43	0.26	1.78
TXS 1616+517	10.11 ± 0.31	2.09 ± 0.09	93.28 ± 4.15	4.34 ± 0.36	0.52 ± 0.02	3.59	0.06	10.79	0.35	0.70	13.11
B3 1343+451	26.55 ± 1.04	2.48 ± 0.04	16.49 ± 1.31	8.67 ± 0.48	0.10 ± 0.01	4.16	0.11	0.42	0.48	1.76	0.68
PKS 2107-105	27.32 ± 1.34	2.30 ± 0.06	7.45 ± 0.90	3.63 ± 0.39	0.67 ± 0.05	9.48	0.0006	17.73	8.30	0.05	150.16

Summary

- **Except for the two BL Lacs, the γ-ray photon index of all the considered high redshift blazars ranges from $2.18\ to\ 3.05$.**
- **The Swift XRT observations show a significant X-ray emission only from the FSRQs considered here The X-ray flux is spanning from $5 \times 10^{-14} erg\ cm^{-2} s^{-1}$ to $10^{-11} erg\ cm^{-2} s^{-1}$.**
- **The γ -ray variability of the considered sources has shown emission on short and long time scales: from sub-day to month scales.**
- **The SEDs were modeled within a one-zone Lepontic scenario, considering the IC scattering of both synchrotron and IR photons from the dusty torus.**
- **The radius of the emitting region is estimated to be $\leq 0.05\, pc$ while the magnetic field and the Doppler factor are correspondingly within $0.10 – 1.74\ G$ and $10.00 – 27.42$. The black hole masses are estimated to be within $(1.69 - 5.35) \times 10^{9} M_{\odot}$.**
- **The jet luminosity is estimated to be $\leq 1.41 \times 10^{46} erg\ s^{-1}$. The jet luminosity is lower than that of the disc $L_D \simeq (1.09 - 10.94) \times 10^{46} erg\ s^{-1}$.**

THANK YOU!!